ISSN 0010-5082, Combustion, Explosion, and Shock Waves, 2018, Vol. 54, No. 6, pp. 642–648. © Pleiades Publishing, Ltd., 2018.
Original Russian Text © A.S. Lobasov, S.S. Abdurakipov, L.M. Chikishev, V.M. Dulin, D.M. Markovich.

HCHO PLIF Investigation of the Flame Shape in an Unsteady Swirling Jet Flow

A. S. Lobasov[a,b], S. S. Abdurakipov[a,b], L. M. Chikishev[a,b], V. M. Dulin[a,b], and D. M. Markovich[a,b]

UDC 536.46

Published in *Fizika Goreniya i Vzryva*, Vol. 54, No. 6, pp. 17–24, November–December, 2018.
Original article submitted August 16, 2017; revision submitted March 6, 2018.

Abstract: This paper describes an experimental study of the spatial structure of the chemical reaction zone in turbulent swirling flames by planar laser-induced fluorescence of formaldehyde (HCHO). Combustion of the methane–air mixture at atmospheric pressure is considered for different values of the equivalence ratio ϕ: inverted cone flames for $\phi = 0.7$ and 1.4 and lifted flames for $\phi = 2.5$. Apart from small-scale deformations, the change in the chemical reaction zone shape is associated with two types of large-scale coherent structures, namely, an almost axisymmetric deformation mode, which appears to be due to the buoyancy effect on the combustion products, and rotation of an asymmetric mode due to the precession of the swirling flow.

Keywords: turbulent swirling flame, coherent structures, planar laser-induced fluorescence, formaldehyde fluorescence, principal component analysis.

DOI: 10.1134/S0010508218060023

INTRODUCTION

Swirling flows are often organized in combustion chambers of gas turbines for flame stabilization. They provide favorable conditions for successful ignition and stable combustion [1, 2]. The structure of turbulent flows with swirling and combustion was investigated in a number of papers [3–5]. Jets with strong swirling are known for the following features of the flow: precessing vortex core (PVC), vortex core breakdown, formation of the central recirculation zone, and nucleation of secondary helical vortices. In recent papers [6–10], large-scale vortex structures and PVC frequency in swirling jets were investigated by means of flow measurements by advanced methods of optical diagnostics and phase (conditional) averaging of the instantaneous velocity and pressure distributions. The impact of the large-scale vortex structures on unsteady combustion regimes in swirling flows has not yet been studied in much detail [11, 12].

Large-scale vortices are known to induce deformations of the flame front, affect the heat release rate, and can result in local flame extinction. These features were studied by using a combination of particle image velocimetry (PIV) and planar-laser induced fluorescence (PLIF) of the hydroxyl [13, 14] produced in the flame front and present in the combustion products. Principal component analysis (PCA) [15] was applied to PIV data to extract coherent structures, similarly to [7, 8] for non-reacting and reacting strongly swirling jets with vortex breakdown. Stöhr et al. [13] found that large-scale vortices improve mixing between the combustion products and fresh mixture. On the other hand, Boxx et al., [14] observed events of local flame extinction during interaction with large-scale vortices, formed in the high-swirl flow. Nevertheless, a detailed analysis of the reaction zone shape and flame front deformations, including those induced by coherent structures of the flow, is desirable.

Formaldehyde (HCHO) is an important combustion intermediate occurring in lower-temperature regions of hydrocarbon flames. It is the initial step of the hydrocarbon oxidation pathway: HCHO → HCO → CO [16]. A high concentration of HCHO serves as a good

[a] Kutateladze Institute of Thermophysics, Siberian Branch, Russian Academy of Sciences, Novosibirsk, 630090 Russia; Alexey.Lobasov@gmail.com.
[b] Novosibirsk State University, Novosibirsk, 630090 Russia.

marker of the preheating zone of hydrocarbon flames. It plays an important role in several combustion processes, including fuel oxidation and self-ignition. Photochemical properties of HCHO have been fairly well studied [17]. One of the more prevalent strategies for HCHO PLIF measurements is the transition excitation by using the third harmonic of Nd:YAG laser radiation at 355 nm [18, 19]. Despite the low intensity of the sideband transition, the energy of the commercially available pulsed Nd:YAG lasers is sufficient for obtaining a sufficiently intense fluorescence signal without using a specific tunable laser.

The present paper reports on the HCHO PLIF investigation of various combustion regimes of the methane–air mixture in a high-swirl turbulent jet with vortex breakdown and the central recirculation zone [8]. The focus is placed on considering large-scale deformations of the reaction zone with the help of the PCA.

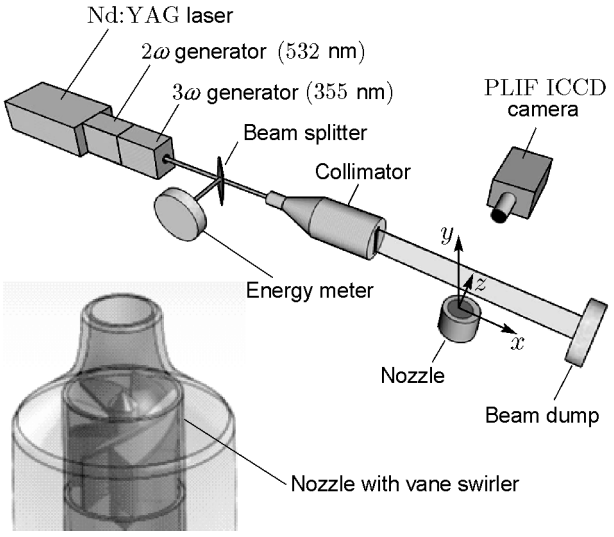

Fig. 1. Sketch of the PLIF setup and nozzle geometry.

EXPERIMENTAL SETUP AND MEASUREMENT TECHNIQUES

The flames are organized in an open combustion rig (see the details in [1]) with a burner consisting of a contracted axisymmetric nozzle (with an exit diameter $d = 15$ mm) with a vane swirler installed inside. The swirl rate based on the definition proposed in [1] is 1.0, which is well above the critical value of 0.6 for vortex breakdown (see [8, 20]). Three values of the equivalence ratio of the methane–air mixture issued from the nozzle are studied: $\phi = 0.7$, 1.4, and 2.5. The jet Reynolds number based on the mean flow rate and viscosity of air is fixed at 5000. The jet bulk velocity without the fuel flow is $U_0 = 5$ m/s.

The layout of the PLIF setup is shown in Fig. 1. The PLIF measurements are carried out for in the longitudinal plane and transverse planes (parallel and perpendicular to the jet axis, respectively) of the flow for different distances from the burner rim. The distance from the burner rim to the measurement plane is varied with accuracy of 100 μm by using a motorized traversing system moving the burner rim along the vertical axis.

The radiation of the third harmonic (355 nm) of the Nd:YAG laser (Quantel Brilliant B with 45 mJ energy per pulse) is used for excitation of HCHO fluorescence. The A–X transition is excited. The root-mean-square (RMS) deviation of the laser pulse energy is below 5%. Collimator optics is used to obtain a light sheet less than 0.8 mm thick in the measurement region. The fluorescence of HCHO is collected by a 16-bit sCMOS camera (LaVision Imager Pro X) equipped with an IRO unit, UV Lens (f#2.8), and an HCHO PLIF optical filter (LaVision). The duration of each laser pulse is approximately 10 ns. The exposure time for each image is 200 ns, and the frame rate is 10 Hz. The images are processed by the DaVis software from LaVision. Raw PLIF images are corrected to take into account the nonuniform intensity of the laser sheet, shot-to-shot variations of the laser energy, and nonuniform sensitivity of the sensor. The background signal is also subtracted.

To reveal the most intense coherent structures in the PLIF images, the PCA is applied to the ensembles of 1000 PLIF snapshots for each type of the flame. The PCA is implemented via the singular value decomposition method [21]:

$$c'(X, Y, t_k) = \sum_{q=1}^{N-1} \alpha_q(t_k)\sigma_q\varphi_q(X, Y), \qquad (1)$$

where

$$\int\limits_{\Omega_{XY}} \varphi_i\varphi_j dX dY = \delta_{ij} \quad \frac{1}{N}\sum_{k=1}^{N} \alpha_i(t_k)\alpha_j(t_k) = \delta_{ij}. \qquad (2)$$

Here δ_{ij} is the Kronecker delta, σ are the singular values (equal to the square roots of the eigenvalues of the covariance matrix of the PLIF images), φ are the spatial distributions of the principal component vectors (eigenvectors of the covariance matrix of the PLIF images), $\alpha_i(t_k)$ are the temporal coefficients of the ith mode, where t_k is the time of kth PLIF image recording, and X and Y are the coordinates of the PLIF images in pixels.

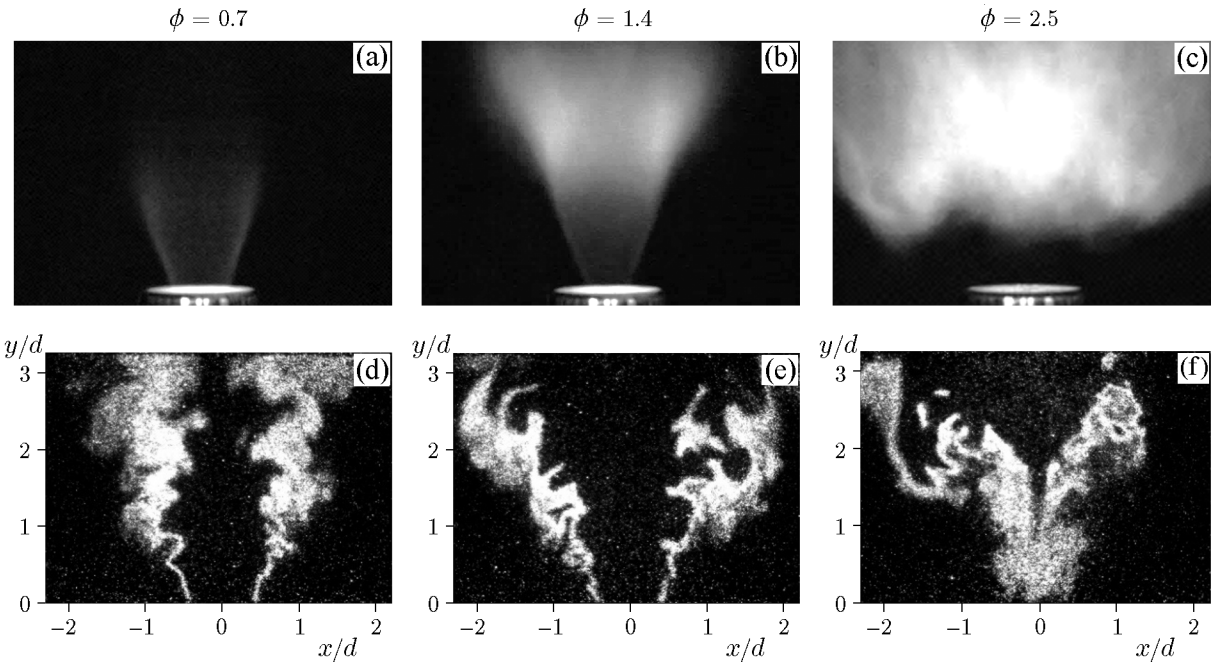

Fig. 2. Photographs of the flames (a–c) and instantaneous HCHO PLIF images of the swirling methane–air flames (d–f) for $\phi = 0.7$ (a and d), 1.4 (b and e), and 2.5 (c and f).

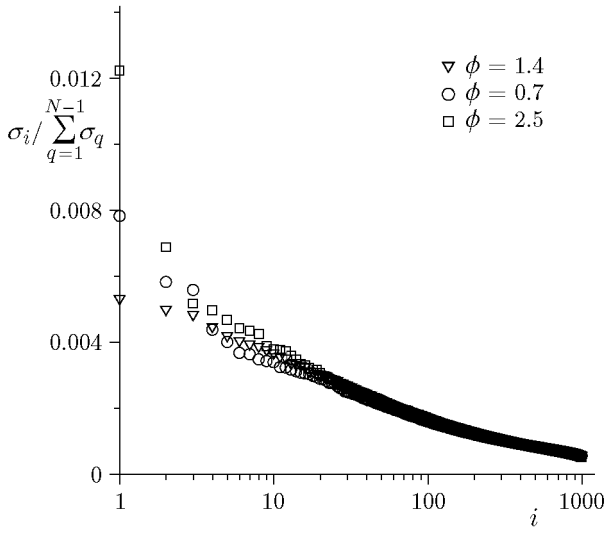

Fig. 3. PCA spectra for the PLIF data in the longitudinal plane of the swirling methane–air flame.

RESULTS

Figure 2 shows the photographs of the flame (with the exposure duration of 1/15 s) and examples of the instantaneous HCHO fluorescence images (captured with an exposure time of 200 ns). The HCHO PLIF images provide information on the spatial structure of the chemical reaction zone in the longitudinal plane, whereas the chemiluminescence on the photograph demonstrates the flame regimes. The gray scale is fixed for all PLIF images.

On the average, flames for the fuel-lean mixture with $\phi = 0.7$ and fuel-rich mixture with $\phi = 1.4$ are shaped as an inverted cone. According to the instantaneous snapshots, the reaction zone undergoes deformations, which become more intense in the downstream

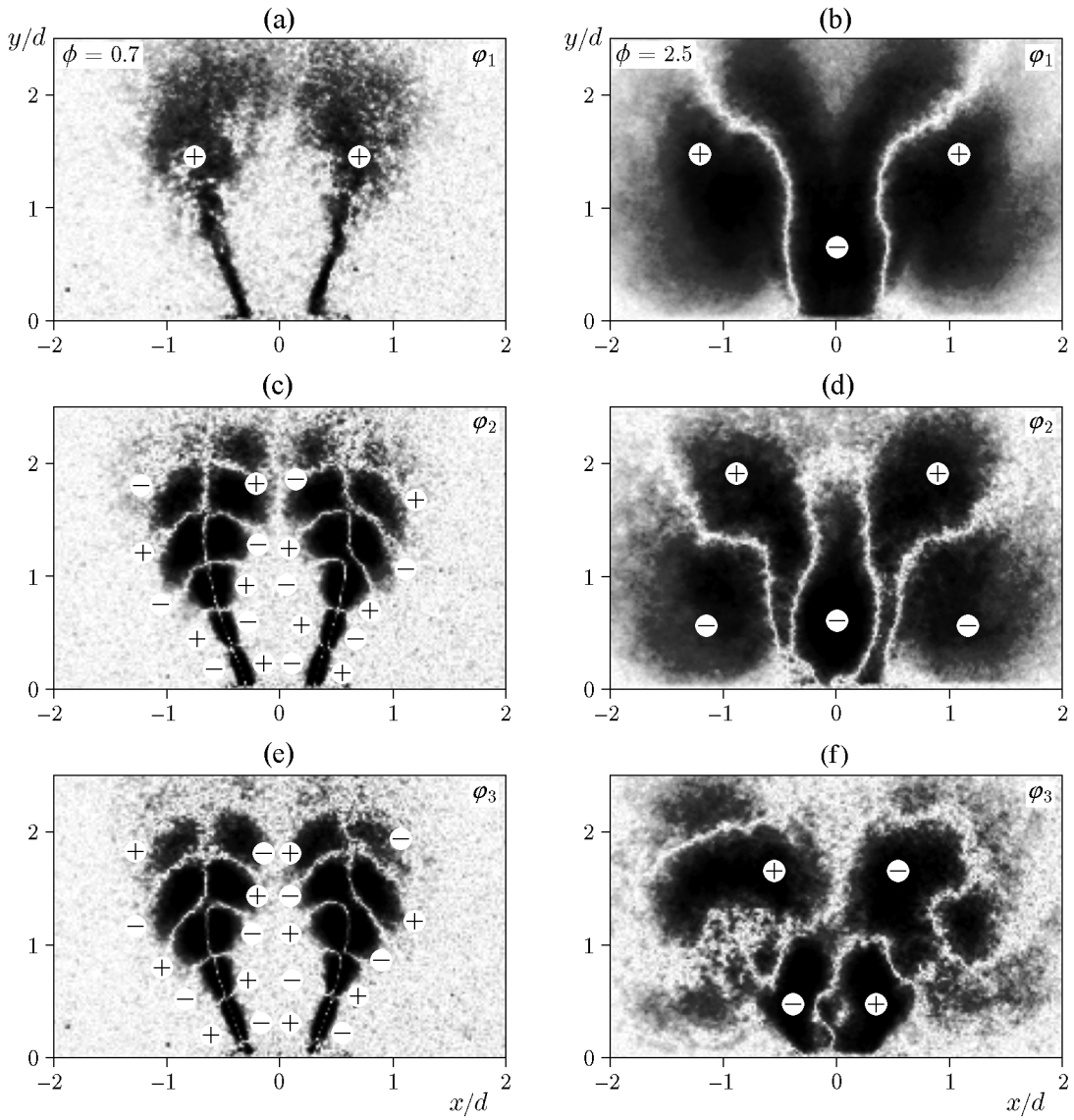

Fig. 4. Spatial distributions for the first three PCA modes: φ_1 (a and b), φ_2 (c and d), and φ_3 (e and f) for HCHO PLIF data in the longitudinal plane of the swirling methane–air flame for $\phi = 0.7$ (a, c, and e) and 2.5 (b, d, and f).

direction. Moreover, individual islands are detected in several instantaneous patterns. The formation of these islands may be caused by two different conditions: out-of-plane closing of the reaction zone or combustion in detached zones, including those trapped by large-scale vortices. The shape of the reaction zone in the case with the fuel-rich lifted flame ($\phi = 2.5$) stabilized at a certain distance downstream from the burner rim differs from the two previous cases. In particular, one can observe HCHO fluorescence around the jet axis for $y/d < 1$. Figure 3 shows the PCA spectra for the PLIF data in the longitudinal plane. For the fuel-rich lifted flame, the amplitude of the first PCA mode is considerably greater than the amplitude of all other modes (by more than twice for $i > 2$).

The spatial distributions of the first three PCA modes are shown in Fig. 4. For the fuel-lean flame ($\phi = 0.7$), the first mode corresponds to oscillations of the PLIF intensity along the mixing layer. The shape of the first mode appears to be roughly symmetrical with respect to the y axis. The second and third PCA modes correspond to spatial deformations in the form of traveling waves along the flame. In both cases, the spatial structures of these modes are asymmetrical relative to the y axis and similar to each other (with a phase shift of $\pi/2$). The PCA modes for the fuel-rich flame

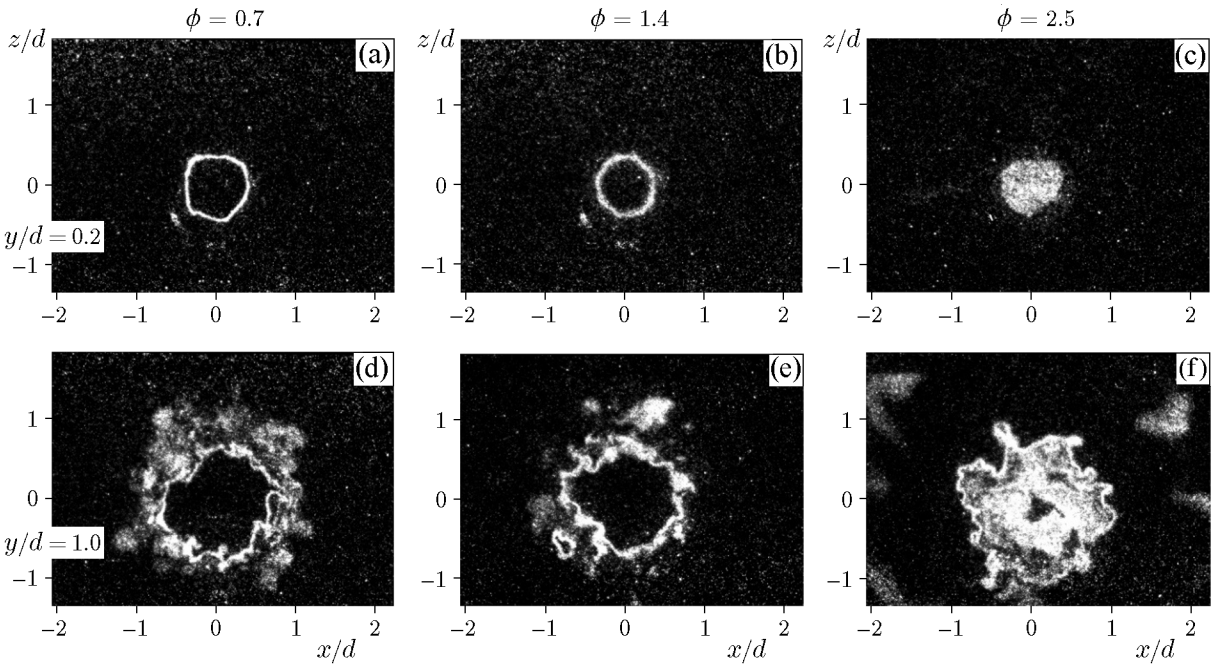

Fig. 5. Examples of the instantaneous HCHO PLIF signal in the transverse planes $y/d = 0.2$ (a–c) and 1.0 (d–f) of the swirling methane–air flame for $\phi = 0.7$ (a and d), 1.4 (b and e), and 2.5 (c and f).

($\phi = 1.4$) also correspond to symmetrical and asymmetrical modes of the reaction zone deformations, which grow downstream, similar to the case of the fuel-lean mixture with $\phi = 0.7$.

The first two PCA modes for the fuel-rich lifted flame with $\phi = 2.5$ correspond to almost symmetrical large-scale oscillations of the PLIF intensity around the y axis and in the mixing layer between the jet and ambient air. The third and fourth PCA modes correspond to disturbances in the form of traveling waves along the jet, which are asymmetric with respect to the y axis.

Examples of the HCHO PLIF data captured in the transverse planes for two different distances from the nozzle are shown in Fig. 5. The example for $y/d = 0.2$ for the case with $\phi = 2.5$ confirms the presence of the reaction zone at the jet axis. In all cases, the reaction zone surface is not axisymmetric because of deformations. The deformations increase in size downstream from the burner. Moreover, smaller individual reaction zone islands can be seen in the transverse planes.

The PCA spectra for the PLIF images in the transverse section $y/d = 1.5$ are shown in Fig. 6. The highest amplitude corresponds to the first PCA mode for the fuel-rich lifted flame with $\phi = 2.5$. According to the spatial distribution shown in Fig. 7, this mode corresponds to the axisymmetric mode of the reaction zone deformations. For the mixtures with $\phi = 0.7$ and 1.4, the first PCA mode also corresponds to almost axisymmetric oscillations of the reaction zone. The second and third PCA modes for the case with $\phi = 2.5$ correspond to a rotating coherent structure, similar to that observed in [11]. It should be noted that the second and third PCA modes for each flame (in the considered region) appear to represent a coherent structure rotated by 90° around the y axis.

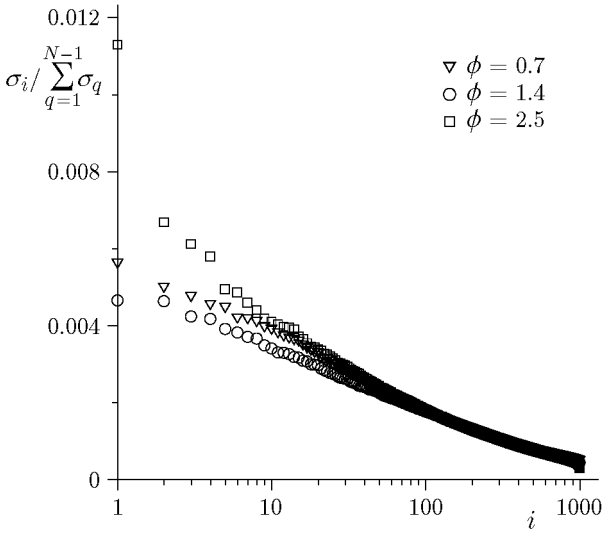

Fig. 6. PCA spectra for the PLIF data in the transverse section $y/d = 1.5$ of the swirling methane–air flame.

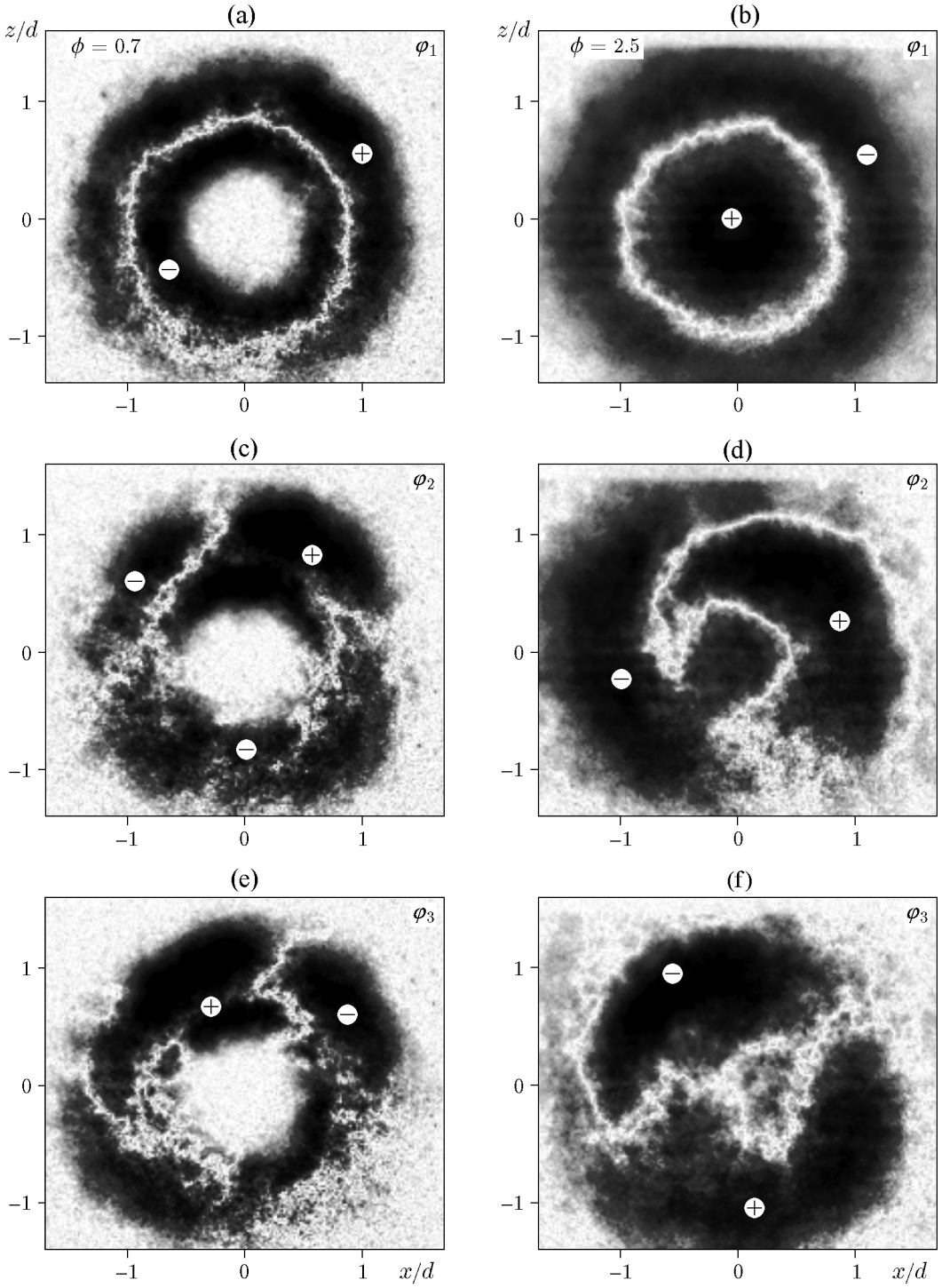

Fig. 7. Spatial distributions of the first three PCA modes: φ_1 (a and b), φ_2 (c and d), and φ_3 (e and f) for the PLIF data in the transverse section $y/d = 1.5$ of the swirling methane–air flame for $\phi = 0.7$ (a, c, and e) and 2.5 (b, d, and f).

CONCLUSIONS

The spatial structure of the chemical reaction zone in the turbulent swirling methane–air flame with vortex core breakdown and precession was studied by planar laser-induced fluorescence of formaldehyde. For the analysis of coherent structures and flame front deformation, the instantaneous data sets were processed by the PCA procedure. Combustion regimes in the form of an inverted cone (lean and rich mixture with equivalence ratio values $\phi = 0.7$ and 1.4) and a lifted flame ($\phi = 2.5$) were considered. Apart from small-scale deformations, it was concluded that the change in the chemical reaction zone shape is associated with two types of large-scale coherent structures, namely, an almost axisymmetric deformation mode, which is presumably due to the buoyancy effect on the combustion products [8, 22], and rotation of the asymmetric mode due to the swirling flow precession.

This work was financially supported by the Russian Science Foundation (Grant No. 16-19-10566).

REFERENCES

1. A. K. Gupta, D. G. Lilley, and N. Syred, *Swirl Flows* (Abacus Press, Kent, 1984).
2. Sh. A. Piralishvili, V. M. Polyaev, and M. N. Sergeev, *Vortex Effect. Experiment, Theory, and Engineering Solutions* (Energomash, Moscow, 2000) [in Russian].
3. S. V. Alekseenko, P. A. Kuibin, and V. L. Okulov, *Introduction into the Theory of Concentrated Vortices* (Kutateladze Inst. of Thermophysics, SB RAS, Novosibirsk, 2003) [in Russian].
4. O. V. Mitrofanova, "Hydrodynamics and Heat Transfer in Swirling Flows in Channels with Swirlers (Analytical Review)," Teplofiz. Vysok. Temp. **41** (4), 587–633 (2003) [High Temp. **41** (4), 518–559 (2003)].
5. A. Y. Varaksin, "Concentrated Air and Fire Vortices: Physical Modeling (A Review)," Teplofiz. Vysok. Temp. **54** (3), 430–452 (2016) [High Temp. **54** (3), 409–427 (2016)].
6. C. E. Cala, E. C. Fernandes, M. V. Heitor, and S. I. Shtork, "Coherent Structures in Unsteady Swirling Jet Flow," Exp. Fluids **40** (2), 267–276 (2006).
7. K. Oberleithner, M. Sieber, N. Nayeri, and C. O. Paschereit, "Three-Dimensional Coherent Structures in a Swirling Jet Undergoing Vortex Breakdown: Stability Analysis and Empirical Mode Construction," J. Fluid Mech. **679**, 383–414 (2011).
8. S. V. Alekseenko, V. M. Dulin, Y. S. Kozorezov, and D. M. Markovich, "Effect of High-Amplitude Forcing on Turbulent Combustion Intensity and Vortex Core Precession in a Strongly Swirling Lifted Propane/Air Flame," Combust. Sci. Technol. **184** (10/11), 1862–1890 (2012).
9. S. Yu. Krasheninnikov, A. K. Mironov, D. E. Pudovikov, and P. D. Toktaliev, "Investigation of the Generation of Sound Waves Produced by Turbulent Jets," Izv. Ross. Akad. Nauk, Mekh. Zhid. Gaza **50** (3), 68–86 (2015) [Fluid Dyn. **50** (3), 371–386 (2015)].
10. I.V. Litvinov, D.K. Sharaborin, and S.I. Shtork, "Finding of Parameters of Helical Symmetry for Unsteady Vortex Flow Based on Phase-Averaged PIV Measurement Data," Teplofiz. Aeromekh. **22** (5), 673–677 (2015) [Thermophys. Aeromech. **22** (5), 647–650 (2015)].
11. N. A. Syred, "Review of Oscillation Mechanisms and the Role of the Precessing Vortex Core (PVC) in Swirl Combustion Systems," Progr. Energy Combust. Sci. **32** (2), 93–161 (2006).
12. T. C. Lieuwen, *Unsteady Combustor Physics* (Cambridge Univ. Press, 2012).
13. M. Stöhr, R. Sadanandan, and W. Meier, "Phase-Resolved Characterization of Vortex–Flame Interaction in a Turbulent Swirl Flame," Exp. Fluids **51** (4), 1153–1167 (2011).
14. I. Boxx, M. Stöhr, C. Carter, and W. Meier, "Temporally Resolved Planar Measurements of Transient Phenomena in a Partially Pre-Mixed Swirl Flame in a Gas Turbine Model Combustor," Combust. Flame **157** (6), 1510–1525 (2010).
15. L. Sirovich, "Turbulence and the Dynamics of Coherent Structures. I. Coherent Structures," Quart. Appl. Math. **45** (3), 561–571 (1987).
16. I. Glassman, *Combustion* (Academic Press, San Diego, 1996).
17. C. Brackmann, J. Nygren, X. Bai, et al., "Laser-Induced Fluorescence of Formaldehyde in Combustion Using Third Harmonic Nd:YAG Laser Excitation," Spectrochim. Acta. A **59** (14), 3347–3356 (2003).
18. J. E. Harrington and K. C. Smyth, "Laser-Induced Fluorescence Measurements of Formaldehyde in Methane/Air Diffusion Flame," Chem. Phys. Lett. **202** (3/4), 196–202 (1993).
19. C. Brackmann, Z. Li, M. Rupinski, N. Docquier, et al., "Strategies for Formaldehyde Detection in Flames an Engines Using a Single-Mode Nd:YAG/OPO Laser System," Appl. Spectrosc. **59** (6), 763–768 (2005).
20. D. M. Markovich, S. S. Abdurakipov, L. M. Chikishev, et al., "Comparative Analysis of Low-and High-Swirl Confined Flames and Jets by Proper Orthogonal and Dynamic Mode Decompositions," Phys. Fluids **24** (6), 065109 (2014).
21. G. Kerschen, J. C. Golinval, A. F. Vakakis, and L. A. Bergman, "The Method of Proper Orthogonal Decomposition for Dynamical Characterization and Order Reduction of Mechanical Systems: An Overview," Nonlin. Dyn. **41** (1), 147–169 (2005).
22. S. S. Abdurakipov, V. M. Dulin, D. M. Markovich, and K. Hanjalic, "Determining Instability Modes in a Gas Flame," Tech. Phys. Lett. **39**, 308–311 (2013).